NASA/CR-1998-208708

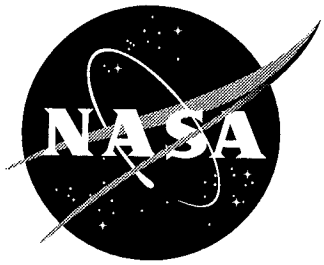

Properties of PZT-Based Piezoelectric Ceramics Between –150 and 250°C

Matthew W. Hooker
Lockheed Martin Engineering & Sciences Co., Hampton, Virginia

National Aeronautics and
Space Administration

Langley Research Center
Hampton, Virginia 23681-2199

Prepared for Langley Research Center
under Contract NAS1-96014

September 1998

Abstract

The properties of three PZT-based piezoelectric ceramics and one PLZT electrostrictive ceramic were measured as a function of temperature. In this work, the dielectric, ferroelectric polarization versus electric field, and piezoelectric properties of PZT-4, PZT-5A, PZT-5H, and PLZT-9/65/35 were measured over a temperature range of -150 to 250°C. In addition to these measurements, the relative thermal expansion of each composition was measured from 25 to 600°C, and the modulus of rupture of each material was measured at room temperature. This report describes the experimental results and compares and contrasts the properties of these materials with respect to their applicability to intelligent aerospace systems.

Keywords: piezoelectric, PZT, PLZT, temperature

Introduction

The term *piezoelectricity* refers to the relationship between pressure and electricity that exists within a unique family of materials. Piezoelectrics are materials that either output a voltage when subjected to a mechanical stress or exhibit a dimensional change when an electric field is applied. These two behaviors are referred to as the direct and indirect modes of operation respectively [1-2]. Both modes of piezoelectric operation are currently being utilized in modern aerospace systems in such diverse applications as vibration cancellation and optical positioning [3-5]. Because these materials have the ability to sense and respond to changes in their environment, they are often referred to as "smart" or "intelligent" materials [6].

The primary applications of piezoelectric technologies in fixed-wing aircraft include the active control of boundary layers along leading edges [7], the suppression of internal cabin noise [8], and the elimination of panel flutter [9] and tail buffeting [10]. This technology is also being applied in helicopters to eliminate the vibrations present in rotor blades [11-13].

In addition to the aeronautical applications of intelligent structures, piezoelectric technologies are also being developed for use in spacecraft systems. In recent years, satellite systems have become smaller and lighter to reduce the cost of launching the payloads into orbit. As spacecraft masses have been reduced, however, the elimination of vibrational disturbances has become a critical design issue. Since many of the scientific instruments aboard these spacecraft require precision pointing to perform their intended functions, the spacecraft must be mechanically stable for the payloads to function as designed. As such, methods of incorporating intelligent structures to minimize jitter in spacecraft structures has become a critical area of research and development in the aerospace community [14-15].

Piezoelectric materials are typically incorporated into aerospace structures by either applying a patch-style device to the surface of the structure [16-17] or by embedding the device into a graphite-epoxy composite structure [18-20]. In each instance, distributed networks of sensors and actuators are used to sense and nullify vibrational disturbances. Similarly-controlled systems are also being developed for use in space-based instruments to actively position optical components [21]. These control systems typically include a position sensor that locates the optical component and a piezoelectric drive mechanism which positions the optic based on real-time feedback from the position sensor.

Because of the wide range of operating conditions for the systems under development, careful consideration must be given to the selection of piezoelectric materials. This is particularly important

when selecting materials for use in systems that will be exposed to a wide range of operating temperatures. To address these concerns, the dielectric, ferroelectric, and electro-mechanical properties of four PZT-based materials were evaluated over a temperature range of -150 to 250°C. Additionally, the thermal expansion properties were measured from 25 to 600°C, and the moduli of rupture were measured at room temperature. This report describes the experimental results and compares and contrasts the properties of the materials evaluated with respect to their applicability to intelligent aerospace systems.

Experimental Procedure

Materials Evaluated

The properties of three piezoelectric materials and one electrostrictive composition were measured between -150 and 250°C. The piezoelectric materials evaluated in this work were commercially-produced PZT-4, PZT-5A, and PZT-5H ceramics. The electrostrictive materials, PLZT-9/65/35, were produced by tape casting powders synthesized by the solid state reaction of PbO, La_2O_3, ZrO_2, and TiO_2. All of the ceramics used in this study were obtained in an unelectroded and unpoled condition and possessed density values that were at least 95% of theoretical density. Prior to testing, gold electrodes were sputtered onto the major surfaces of each specimen.

Initially, the room temperature (25°C) dielectric, ferroelectric, and piezoelectric properties of each composition were determined. Once the initial room temperature evaluations were complete, the properties of each composition were then measured between -150 and 250°C. The specific details of each measurement are described below.

During the thermal tests, each specimen was placed in an environmental chamber with a temperature sensor located in close proximity to the test article. Throughout this investigation, multiple specimens of each composition were tested at each condition, and the average value of each property was determined.

Dielectric and Ferroelectric Measurements

The dielectric constant (K), dissipation factor (tan δ), and electrical resistivity of each composition were measured at frequencies of 100 Hz, 1 kHz, 10 kHz, and 100 kHz using an HP 4284A LCR meter. From this data, the Curie point (T_c) of each specimen exhibiting a maximum dielectric constant between -150 and 250°C was determined.

Next, the ferroelectric polarization versus electric field (P-E) properties of each composition were measured at 1 Hz using a Sawyer-Tower circuit. The P-E properties of the soft piezoelectric materials (i.e., PZT-5A and PZT-5H), as well as the electrostrictive specimens, were measured in an unpoled condition. However, because the hard piezoelectric ceramics (i.e., PZT-4) are not initially polarizable at room temperature, these specimens were poled at 100°C prior to testing. The properties of these materials were tested in the polarized state in order to accurately simulate the polarization state of the materials as they would be used in practice.

Piezoelectric Measurements

The piezoelectric coefficients of each composition were measured in accordance with published standards [22-23]. The various specimen geometries and electrode patterns necessary for determining the piezoelectric coefficients for radial, transverse, and longitudinal modes of operation are shown in Figure 1. The circular ceramics used in this work were 25.4 mm in diameter and 250 to 380 μm thick. The rectangular specimens had dimensions 2 mm x 2 mm x 7.5 mm.

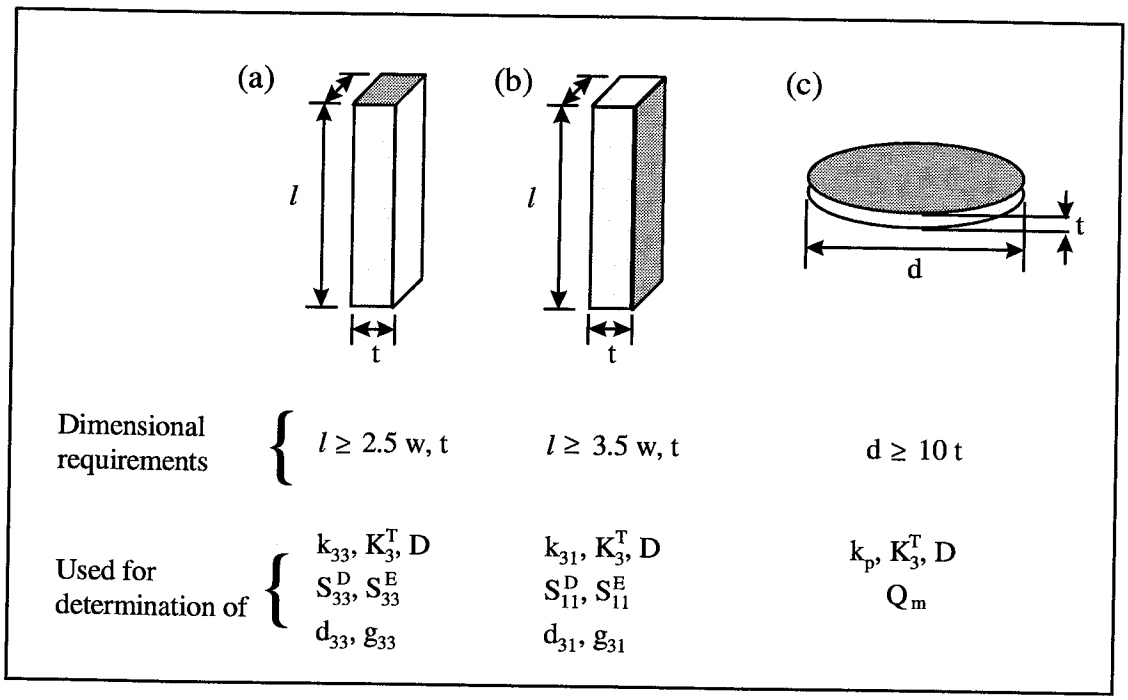

Figure 1. Specimen geometries and polarization directions associated with the measurement of radial, transverse, and longitudinal piezoelectric properties.

The resonance properties of the poled piezoelectric specimens were measured using an HP 4194A Impedance Analyzer. The effective electromechanical coupling coefficient, k_{eff}, of the radial test specimens was then calculated using the resonance/antiresonance method described by the relation [23]:

$$k_{eff} = \sqrt{\frac{f_n^2 - f_m^2}{f_n^2}} \tag{1}$$

where f_m and f_n refer to the frequencies of minimum and maximum impedance, respectively. In addition to the k_{eff} values, the planar coupling coefficient, k_p, for each composition was determined using the procedures described in references 22 and 23.

The piezoelectric coefficients for the transverse (k_{31}, d_{31}, and g_{31}) and longitudinal (k_{33}, d_{33}, and g_{33}) modes of operation were determined by measuring the resonance properties of the thickness-poled and length-poled ceramics, respectively. The coefficients describing the transverse mode of operation were calculated using the following relations:

$$k_{31} = \sqrt{\frac{A}{1+A}} \tag{2}$$

where $$A = \frac{\pi}{2}\frac{f_m}{f_n}\tan\frac{\pi}{2}\frac{(f_n - f_m)}{f_m} \tag{3}$$

$$S_{11}^{E} = \frac{1}{4\rho f_m^2 l^2} \tag{4}$$

$$d_{31} = k_{31}\sqrt{\varepsilon_0 K_3 S_{11}^{E}} \tag{5}$$

$$g_{31} = \frac{d_{31}}{\varepsilon_0 K_3} \tag{6}$$

The coefficients for the longitudinal mode of operation were calculated using the relations:

$$k_{33} = \sqrt{\frac{\pi}{2}\frac{f_m}{f_n}\tan\frac{\pi}{2}\frac{(f_n - f_m)}{f_n}} \tag{7}$$

$$S_{33}^{D} = \frac{1}{4\rho f_n^2 l^2} \tag{8}$$

$$S_{33}^{E} = \frac{S_{33}^{D}}{1 - k_{33}^2} \tag{9}$$

$$d_{33} = k_{33}\sqrt{\varepsilon_0 K_3 S_{33}^{E}} \tag{10}$$

$$g_{33} = \frac{d_{33}}{\varepsilon_0 K_3} \tag{11}$$

All of the symbols used in equations 1-11 are defined in Table 1.

Table 1. Definition of symbols used in the determination of piezoelectric coefficients.

Symbol	Definition	Units
d_{31}	Transverse strain constant	m/V
d_{33}	Extensional strain constant	m/V
D (superscript)	At constant electric displacement	
E (superscript)	At constant electric field	
f_m	Frequency of minimum impedance	Hz
f_n	Frequency of maximum impedance	Hz
g_{31}	Transverse voltage constant	V m/N
g_{33}	Extensional voltage constant	V m/N
k_{31}	Transverse coupling coefficient	
k_{33}	Extensional coupling coefficient	
k_{eff}	Effective electro-mechanical coupling coefficient	
k_p	Planar coupling coefficient	
K_3	Dielectric constant	
l	Specimen length	m
S_{11}, S_{33}	Elastic compliance constants	m^2/N
ε_0	Permittivity of free space, 8.85×10^{-12}	F/m
ρ	Density	kg/m^3

Thermal Expansion Measurements

The thermal expansion properties of unelectroded, unpoled specimens with dimensions 25 mm x 4 mm x 3 mm were measured from 25 to 600°C using a Linseis model L75 dilatometer. All of these tests were performed in an argon atmosphere using a heating rate of 2°C/min. Once the measurements were complete, the relative change in length, $\Delta l/l_0$, for each material was calculated.

Mechanical Testing

The flexural strength of each composition was measured at room temperature using a four-point bend test. In this work, unelectroded and unpoled ceramics with dimensions of 38 mm x 6 mm x 4 mm were tested to failure. All of the mechanical testing was performed using a load rate of 0.25 mm/min and inner and outer span lengths of 17 and 34 mm, respectively. Once all of the tests were complete, the Modulus of Rupture (MOR) of each specimen was calculated using the relation [24]:

$$\mathrm{MOR} = \frac{3\mathrm{P}(\mathrm{L}-a)}{2bd^2} \tag{12}$$

where P is the mechanical load required to break the specimen, L is the outer span distance, a is the inner span distance, b is the width of the bar, and d is the depth of the bar. Between five and ten specimens of each composition were tested, and an average MOR value was calculated for each composition.

Experimental Results

Room Temperature Properties

As shown in Table 2, all of the materials evaluated in this work possessed room-temperature dielectric constants ranging from 1100 to 5000. Additionally, each of the piezoelectric compositions exhibited E_C and P_R values in excess of 5.5 kV/cm and 12.9 $\mu C/cm^2$, whereas the electrostrictive possessed E_C and P_R values of 2.5 kV/cm and 1.1 $\mu C/cm^2$, respectively.

After the initial dielectric and ferroelectric measurements were performed, additional materials of each composition were poled and tested. The piezoelectric specimens exhibited k_{eff} values ranging from 0.49 to 0.53, with the highest values exhibited by the PZT-5H ceramics. The PZT-5H ceramics also exhibited the highest d_{31} and d_{33} values followed by the PZT-5A and PZT-4 compositions, respectively. Because of the cubic nature of the PLZT-9/65/35 crystal structure, these materials do not exhibit strong resonance properties, and therefore, the calculation of piezoelectric coefficients for these materials yields negligible values.

Table 2. Room temperature (25°C) dielectric, ferroelectric, and piezoelectric properties of PZT-based ceramics.

Property	Units	PZT-4	PZT-5A	PZT-5H	PLZT-9/65/35
K (1 kHz)	---	1400	1600	3400	5000
tan δ (1kHz)	---	0.05	0.02	0.02	0.06
E_C	kV/cm	14.4	11.8	5.5	2.5
P_R	μC/cm^2	31.0	23.0	12.9	1.1
P_{SAT}	μC/cm^2	40.1	27.7	19.5	20.8
k_{eff}	---	0.49	0.50	0.53	---
k_p	---	0.54	0.56	0.59	---
d_{33} (x10^{-12})	m/V	225	350	585	---
g_{33} (x10^{-3})	Vm/N	8.5	16.6	12.5	---
k_{33}	---	0.35	0.53	0.59	---
d_{31} (x10^{-12})	m/V	-85	-190	-265	---
g_{31} (x10^{-3})	Vm/N	-7.5	-13.7	-8.5	---
k_{31}	---	0.22	0.40	0.36	---
Density	g/cm^3	7.6	7.7	7.4	7.3

Dielectric and Resistive Properties

As shown in Figure 2, all of the materials evaluated in this work exhibited their lowest dielectric constant values at -150°C, and as the temperature was increased the dielectric constant of each composition also increased. The dielectric constants of the PZT-4 and PZT-5A ceramics increased steadily as a function of temperature with neither possessing a Curie point in the temperature range evaluated in this study. The other two materials evaluated, PZT-5H and PLZT-9/65/35, exhibited Curie points within the -150 to 250°C range. The PZT-5H ceramics possessed a T_c value of 180°C at each frequency, whereas the PLZT-9/65/35 materials exhibited T_c properties typical of a relaxor ferroelectric (i.e., varying with frequency). In this instance, the temperature at which the maximum dielectric constant was observed increased from 72 to 91°C as the measurement frequency increased from 100 Hz to 100 kHz.

The dissipation factors for each material were also found to be dependent upon both the temperature and measurement frequency. As shown in Figure 3, the tan δ values for PZT-4 were approximately 0.05 over the entire temperature range when measured at 10 and 100 kHz. At 100 Hz and 1 kHz, however, the dissipation factor began to increase at 125 and 150°C, respectively. The tan δ values for PZT-5A were also found to be relatively constant when measured at frequencies of 100 Hz, 1 kHz, and 10 kHz. However, at 100 kHz the dielectric loss was significantly higher over the entire temperature range.

Unlike the previous two materials discussed, the PZT-5H and PLZT-9/65/35 ceramics exhibited maximum tan δ values at each measurement frequency which correspond to their respective Curie points. In both instances, the dissipation factors were found to increase with increasing measurement frequency as seen in Figures 3 (c) and 3 (d).

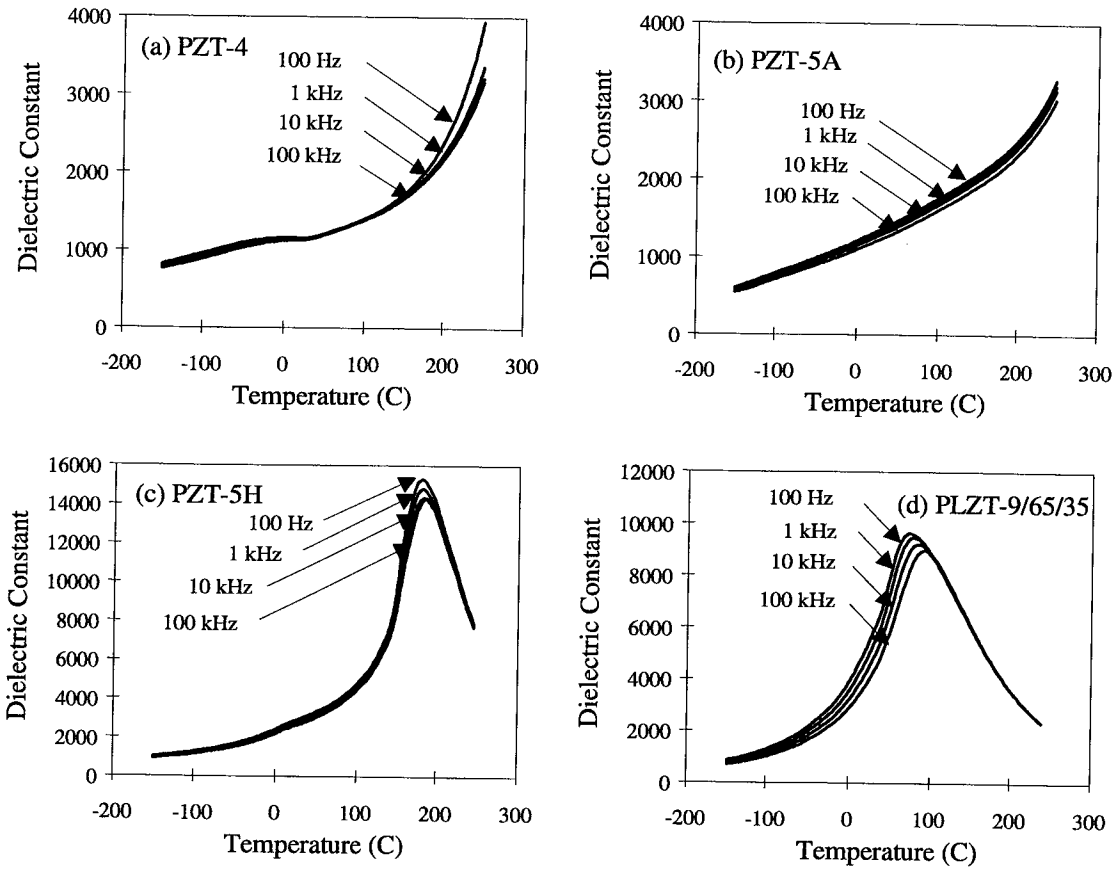

Figure 2. Dielectric constant versus temperature data for (a) PZT-4, (b) PZT-5A, PZT-5H, and (d) PLZT-9/65/35.

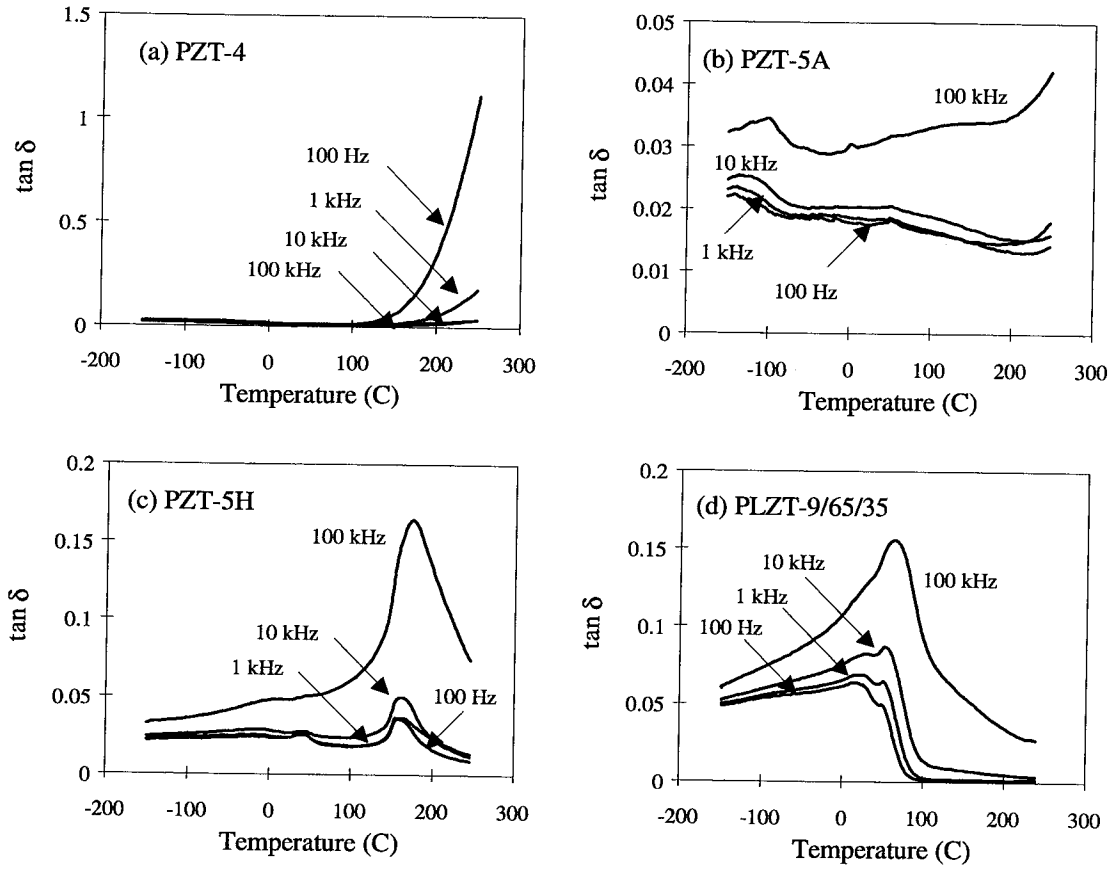

Figure 3. Dissipation factor (tan δ) versus temperature data for (a) PZT-4, (b) PZT-5A, PZT-5H, and (d) PLZT-9/65/35.

As shown in Figure 4, the resistivity of the PZT-4 ceramics remained relatively constant between -150 and 50°C. However, as the temperature was further increased the resistivity was found to decrease significantly. For example, the resistivity measured at 100 Hz decreased from 10^9 Ω-cm at 50°C to less than 10^7 Ω-cm at 250°C. The PZT-5A ceramics were also found to possess a resistivity on the order of 10^9 Ω-cm at -150°C when measured at 100 Hz. Although the resistivity of the PZT-5A specimens was found to decrease with increasing temperature, these materials did not exhibit the sharp decrease in resistivity exhibited by the PZT-4 ceramics as the measurement temperature exceeded 50°C.

The resistivity of the PZT-5H materials was also found to decrease with increasing temperature. In this instance, however, the resistance reached a minimum value at the Curie point and increased as the test specimen was heated to 250°C. A resistance minimum corresponding to the Curie temperature was also observed for the PLZT-9/65/35 ceramics. As previously noted, this material is a relaxor ferroelectric and therefore the temperature of minimum resistance was found to increase from 72 to 91°C as the measurement frequency increased from 100 Hz to 100 kHz.

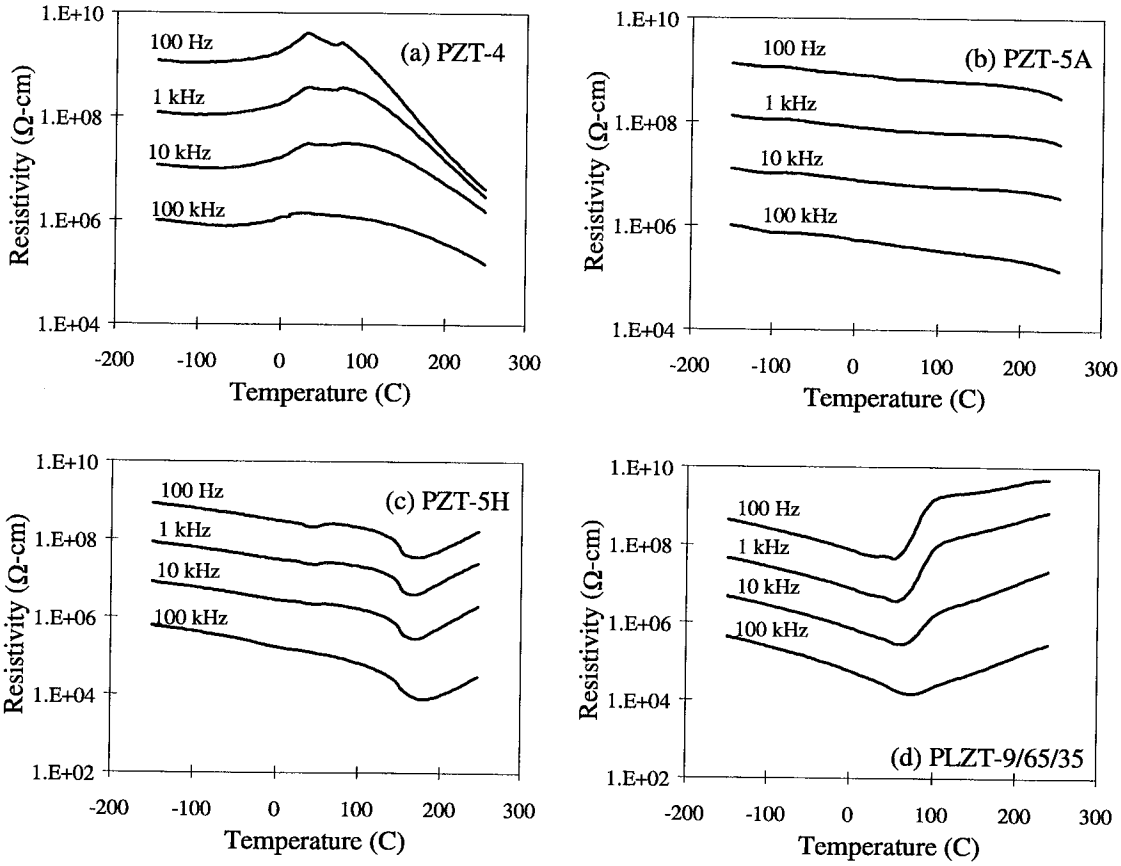

Figure 4. Resistivity versus temperature data for (a) PZT-4, (b) PZT-5A, (c) PZT-5H, and (d) PLZT-9/65/35.

Ferroelectric Polarization versus Electric Field Properties

As shown in Figures 5 (a) to 5 (c), all of the piezoelectric ceramics evaluated in this work possessed maximum remanent polarization values between 0 and 50°C, indicating that the highest induced polarization states occur near room temperature. For each composition tested, the P_R values were lowest

at -150°C and increased until a maximum value was reached. As the temperature was further increased beyond the temperature at which the maximum value was observed, the P_R values of each composition decreased steadily over the balance of the temperature range.

As previously mentioned, the resistivity of the PZT-4 materials decreased as the materials were heated beyond 50°C. Because of this decrease in resistance, calculation of the P_R values at temperatures above 120°C indicates an increase that is due to the conductive nature of these materials at high temperatures. The increase in the P_R and P_{SAT} values above 120°C is illustrated in Figure 5 (a). As the temperature was further increased, the application of high electric fields ultimately led to the breakdown of these specimens. Therefore, P-E data for this material was not collected above 160°C.

Unlike the PZT-4 specimens, the PZT-5A ceramics were polarizable over the entire temperature range. As shown in Figure 5 (b), the P_R values for this composition increased from 2 $\mu C/cm^2$ at -150°C to a maximum value of 25 $\mu C/cm^2$ at 25°C. As the temperature was further increased to 250°C, the P_R values decreased to 20 $\mu C/cm^2$.

As shown in Figures 5 (c) and 5 (d), the P_R values for both PZT-5H and PLZT-9/65/35 reached maximum values near 25°C and then decreased steadily with increasing temperature until the material no longer exhibited a ferroelectric hysteresis. Each of these latter compositions exhibited paraelectric P-E behaviors at each measurement temperature above their respective T_c values.

The coercive field values for each composition were also found to exhibit a maximum value and then decrease with increasing temperature. As seen in Figures 5 (a) to 5 (d), the maximum coercive field values were found to occur between -100 and -50°C. As was noted in the P_R behaviors, the E_C values for the PZT-5H and PLZT-9/65/35 materials decreased to zero at their respective Curie points, indicating that the ferroelectric domains are not spontaneously reversible and that a remanent polarization state can not be induced above that temperature.

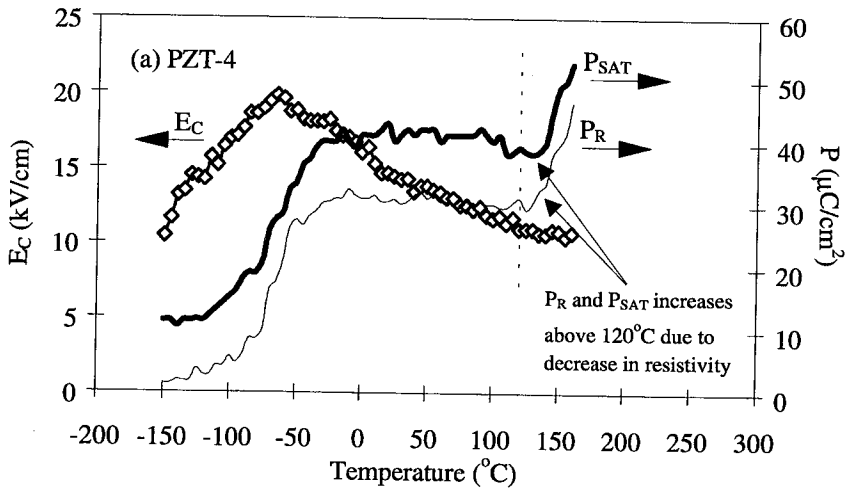

Figure 5. Coercive field (E_C), remanent polarization (P_R), and saturation polarization (P_{SAT}) versus temperature properties of (a) PZT-4, (b) PZT-5A, (c) PZT-5H, and (d) PLZT-9/65/35.

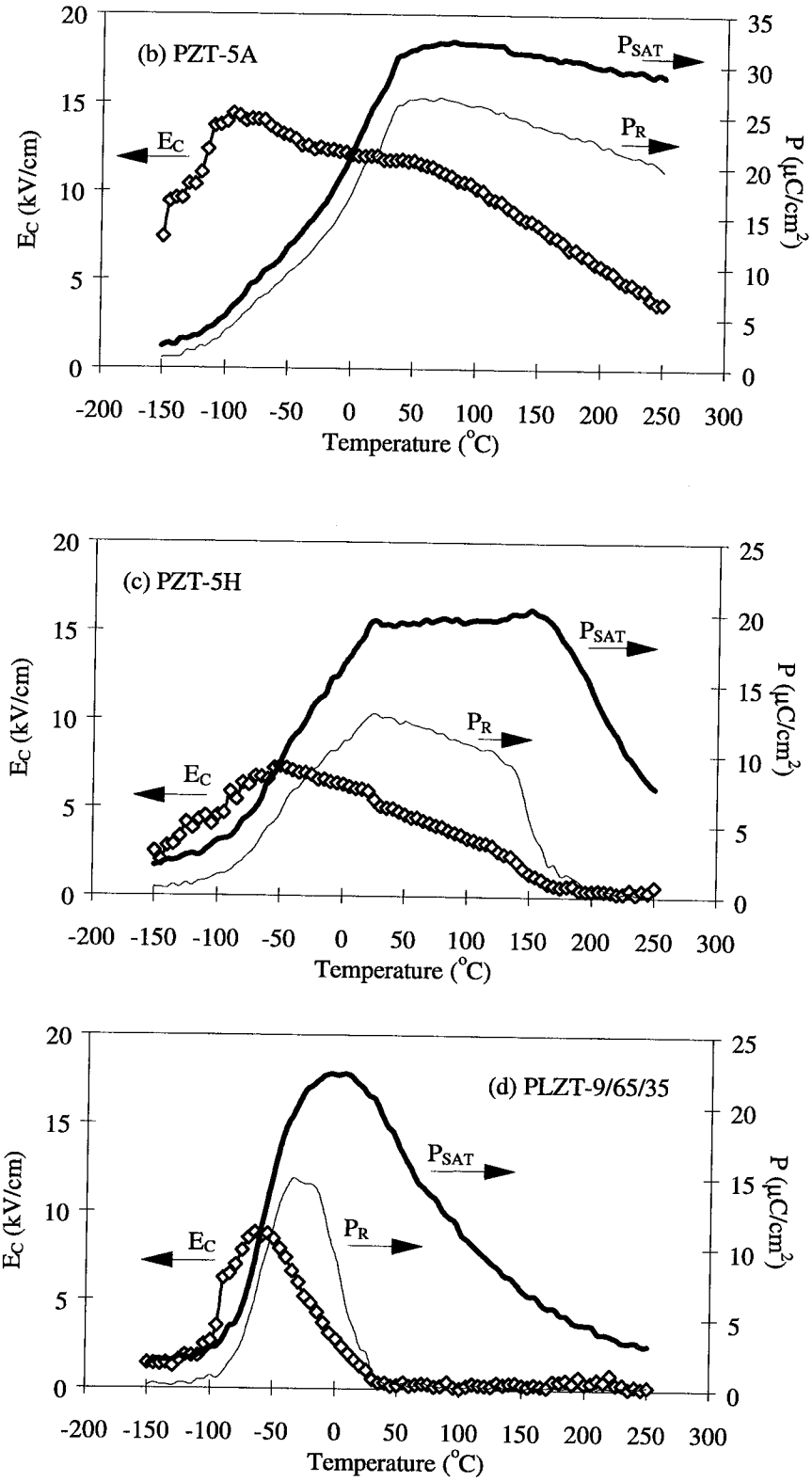

Figure 5 (continued). Coercive field (E_C), remanent polarization (P_R), and saturation polarization (P_{SAT}) versus temperature properties of (a) PZT-4, (b) PZT-5A, (c) PZT-5H, and (d) PLZT-9/65/35.

In addition to the graphs summarizing the ferroelectric hysteresis properties of each composition from -150 to 250°C, typical examples of the P-E behaviors of each composition at -150, -75, 0, 25, 100, and 250°C are shown in Figures 6 to 9. As previously discussed, each composition exhibits a very low polarization of -150°C, and as the temperature increases, the hysteresis loops of the three piezoelectric compositions exhibit typical square (PZT-4 and PZT-5A) or rounded (PZT-5H) ferroelectric hysteresis behavior near room temperature.

As shown in Figures 6 (a) and 6 (b), the PZT-4 ceramics exhibited somewhat asymmetric hysteresis behavior below -50°C. However, all of the P-E loops collected above this temperature were symmetric about each axis. Symmetric hysteresis loops were obtained at every temperature for the soft piezoelectric ceramics evaluated herein.

The PLZT-9/65/35 ceramics also exhibited low polarization properties at -150°C. However, as previously observed in Figure 5 (d), the maximum E_C and P_{SAT} values for this composition were obtained near -50°C. At this temperature, these materials exhibit a P-E behavior that is very similar to those of the piezoelectric ceramics near room temperature. As these specimens were further heated to 25°C, the remanent polarization and coercive field values decreased significantly, and a slim-loop ferroelectric behavior was observed at room temperature (see Figure 9 (d)).

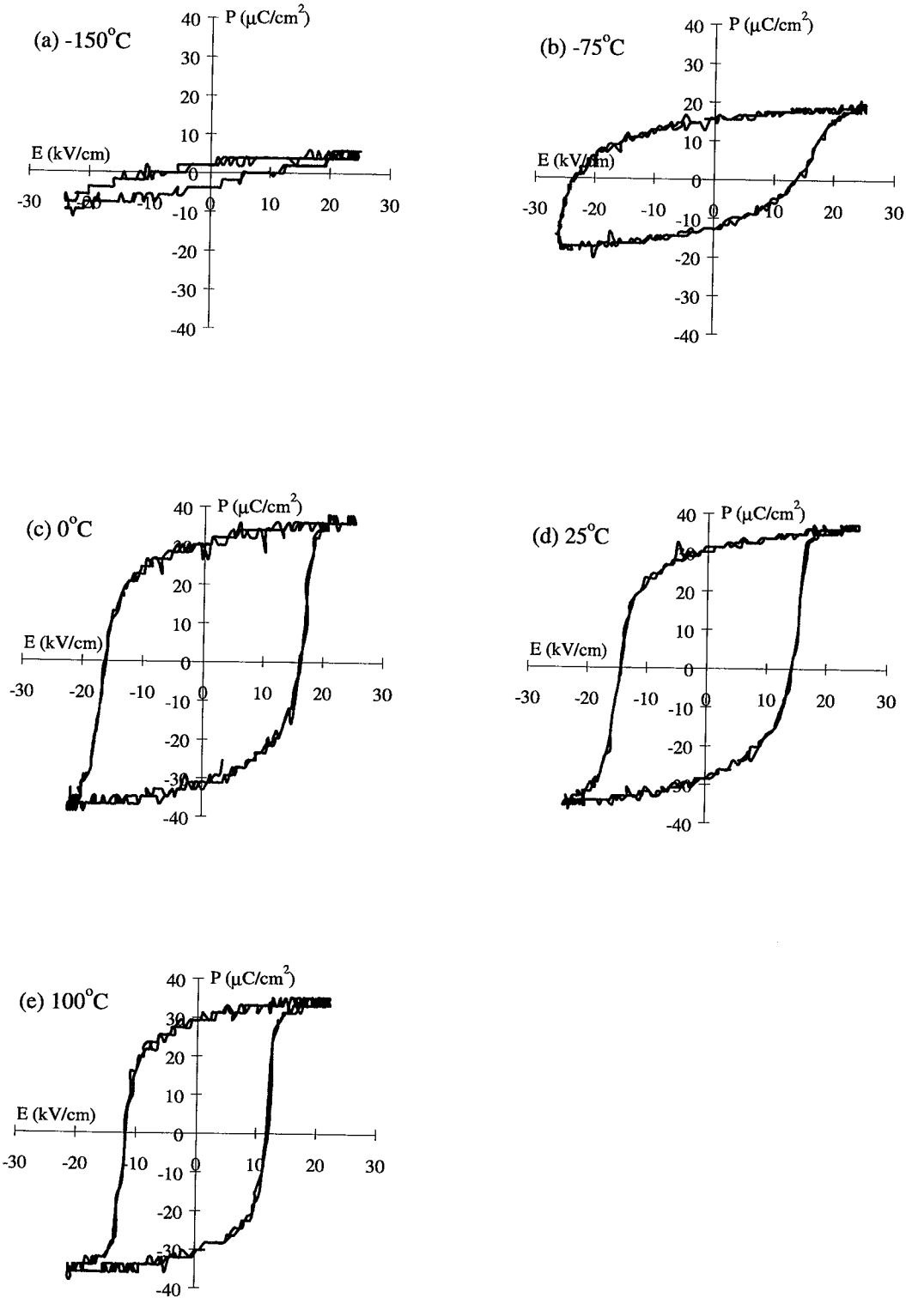

Figure 6. Typical ferroelectric polarization versus electric field (P-E) properties of PZT-4 ceramics at (a) -150°C, (b) -75°C, (c) 0°C, (d) 25°C, (e) 100°C, and (f) 150°C.

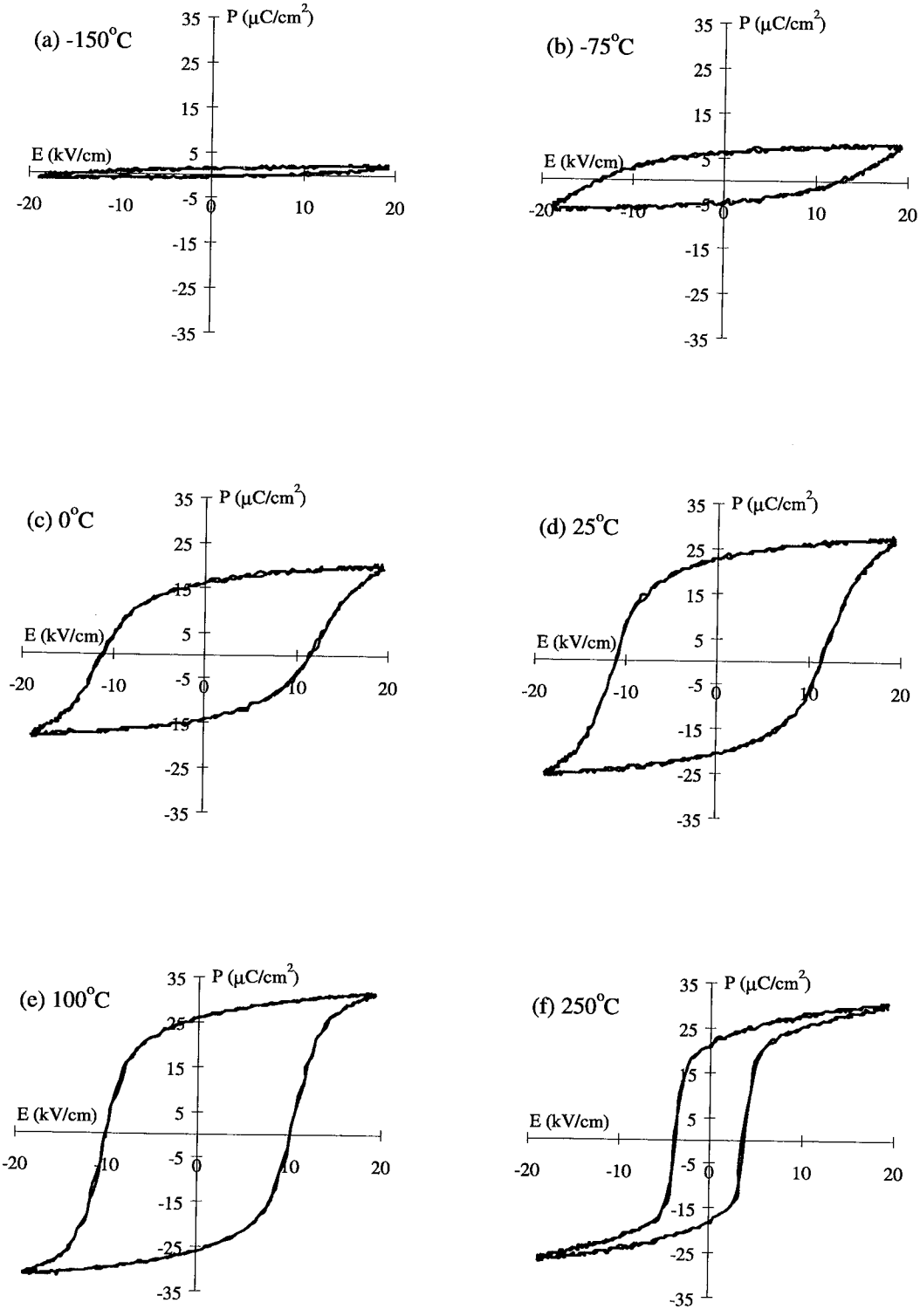

Figure 7. Typical ferroelectric polarization versus electric field (P-E) properties of PZT-5A ceramics at (a) -150°C, (b) -75°C, (c) 0°C, (d) 25°C, (e) 100°C, and (f) 250°C.

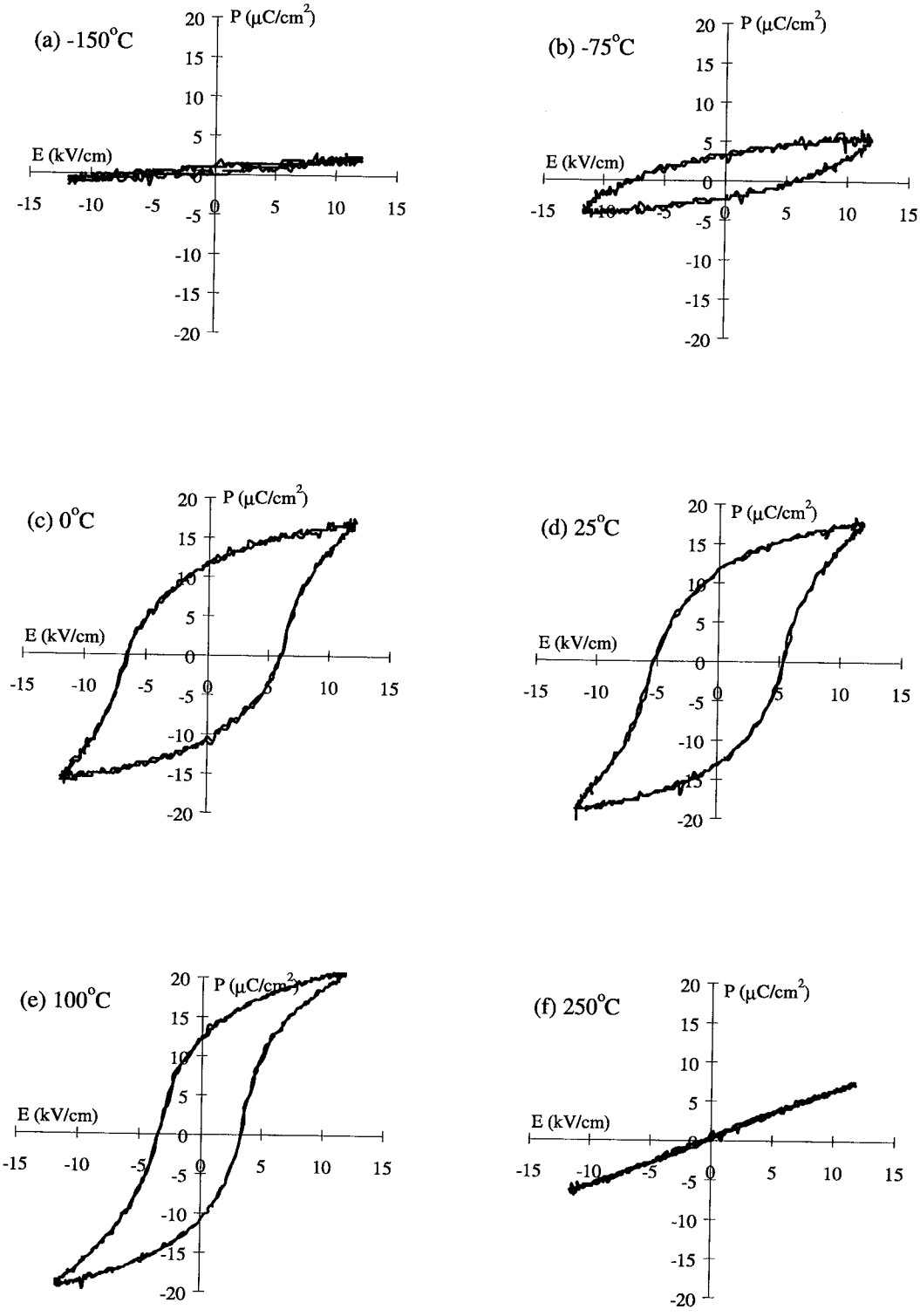

Figure 8. Typical ferroelectric polarization versus electric field (P-E) properties of PZT-5H ceramics at (a) -150°C, (b) -75°C, (c) 0°C, (d) 25°C, (e) 100°C, and (f) 250°C.

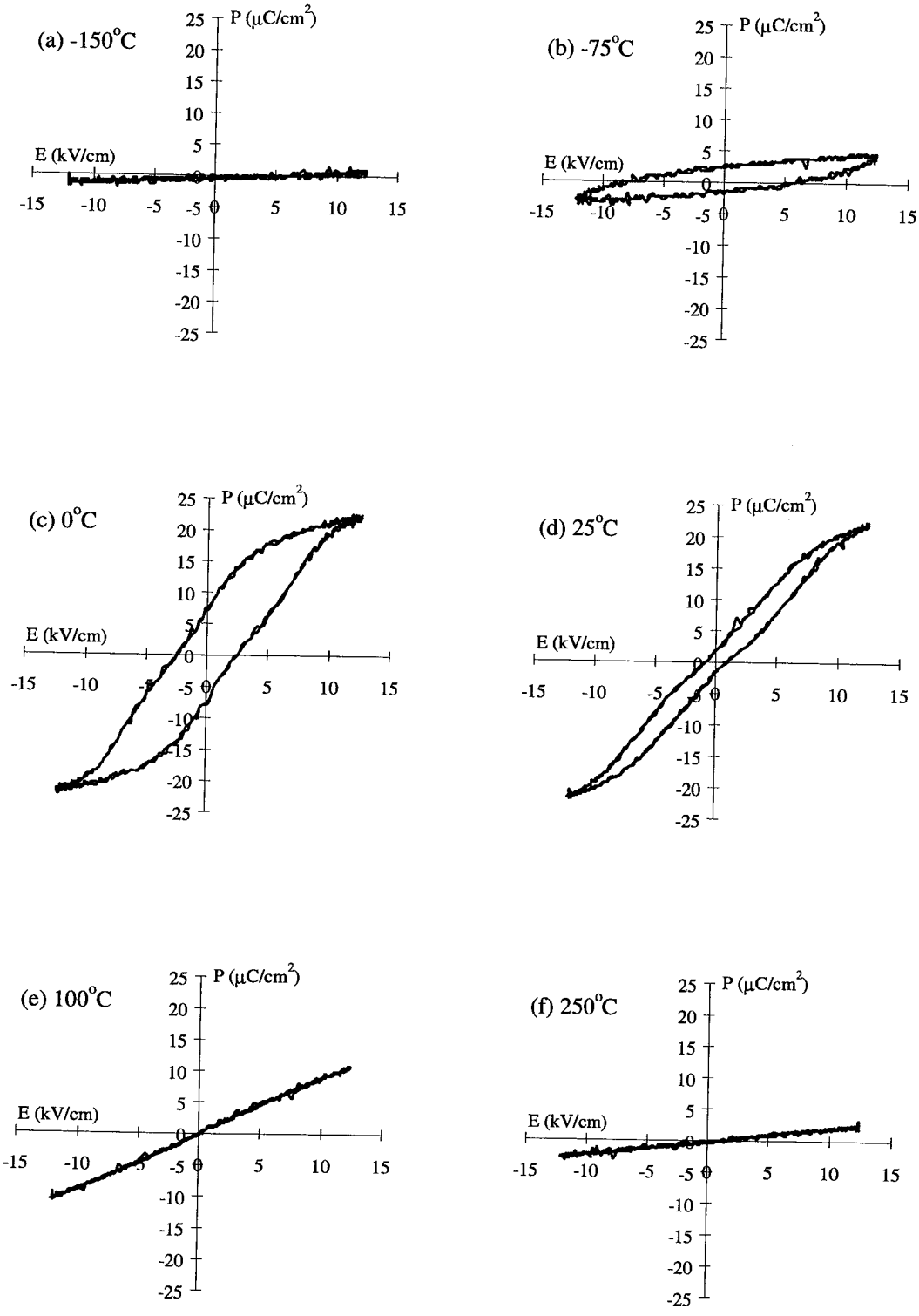

Figure 9. Typical ferroelectric polarization versus electric field (P-E) properties of PLZT-9/65/35 ceramics at (a) -150°C, (b) -75°C, (c) 0°C, (d) 25°C, (e) 100°C, and (f) 250°C.

Piezoelectric Properties

As previously mentioned, the PZT-5H ceramics exhibited the highest piezoelectric properties (i.e., k_{eff}, k_p, $|d_{31}|$, and d_{33}) at room temperature, followed by the PZT-5A and PZT-4 materials, respectively. When cooled to -150°C, the k_{eff} and k_p values of each composition remained relatively constant. The $|d_{31}|$ and d_{33} values for PZT-4 also remained relatively stable over this temperature range. The d constants for the PZT-5A and PZT-5H ceramics, however, decreased to approximately 50% of their room temperature values when cooled to -150°C.

When heated to 250°C, the electro-mechanical coupling coefficients of PZT-4 and PZT-5A decreased from their room temperature values, whereas the d constants for these materials increased over this temperature interval. The properties of the PZT-5H specimens exhibited similar trends when heated above room temperature. However, in this instance the specimens no longer exhibited measurable resonances above 170°C, thereby indicating that the specimens had been thermally de-poled.

As shown in Figure 10 (a), each of the piezoelectric compositions possessed a k_{eff} value ranging from 0.45 and 0.55 between -150 and 150°C. Above 150°C, the k_{eff} value of each composition began to decrease, with the PZT-5H ceramics becoming completely de-poled at 170°C. The PZT-4 and PZT-5A specimens both exhibited minimum k_{eff} values at 250°C. In this work, minimum k_{eff} values of 0.38 and 0.44 were obtained at 250°C for the PZT-4 and PZT-5A ceramics, respectively.

Similar trends were also observed in the measured k_p values. As seen in Figure 10 (b), the k_p values of each composition were between 0.5 and 0.6 over the -150 to 150°C temperature interval. Furthermore, the k_p values of the PZT-4 and PZT-5A ceramics decreased to minimum values of 0.40 and 0.48 at 250°C. Likewise, above 150°C, the k_p values for the PZT-5H ceramics decreased sharply to zero near 170°C.

As shown in Figures 11 (a) and (b), each composition exhibited its minimum $|d_{31}|$ and d_{33} values at -150°C. At -150°C, the d constants of the PZT-4 ceramics decreased less than 10% from their room temperature values whereas the properties of the PZT-5A and PZT-5H compositions declined by approximately 50% over the same temperature interval. Although PZT-4 ceramics exhibited the most stable performance between -150 to 25°C, the d_{33} values for this composition are significantly lower than those of the other two piezoelectric materials near room temperature.

When the materials were heated from 25 to 250°C, the d_{33} values of the PZT-4 and PZT-5A ceramics increased continuously to their maximum values whereas the properties of the PZT-5H ceramics were more strongly dependent upon the measurement temperature. Specifically, the PZT-4 and PZT-5A ceramics exhibited maximum d_{33} values of 360×10^{-12} and 440×10^{-12} m/V at 250°C whereas the PZT-5H specimens possessed d_{33} values on the order of 900×10^{-12} m/V before being thermally de-poled at approximately 170°C.

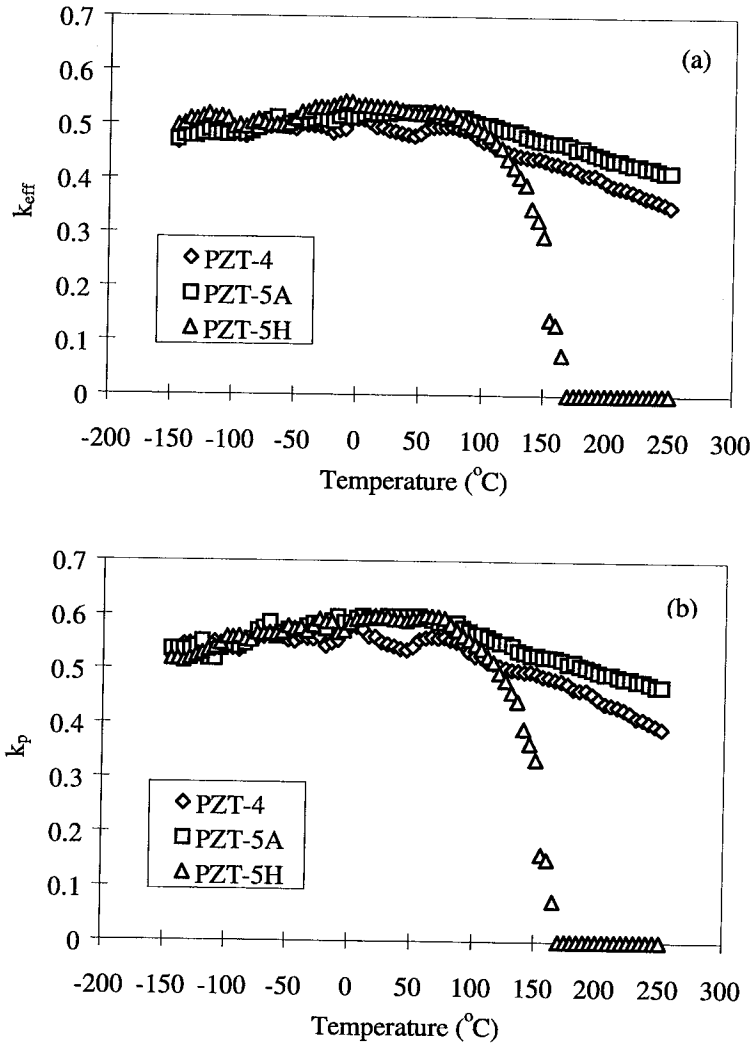

Figure 10. Typical (a) effective electro-mechanical coupling coefficient (k_{eff}) and (b) planar coupling coefficient (k_p) versus temperature behavior of PZT-4, PZT-5A, and PZT-5H ceramics.

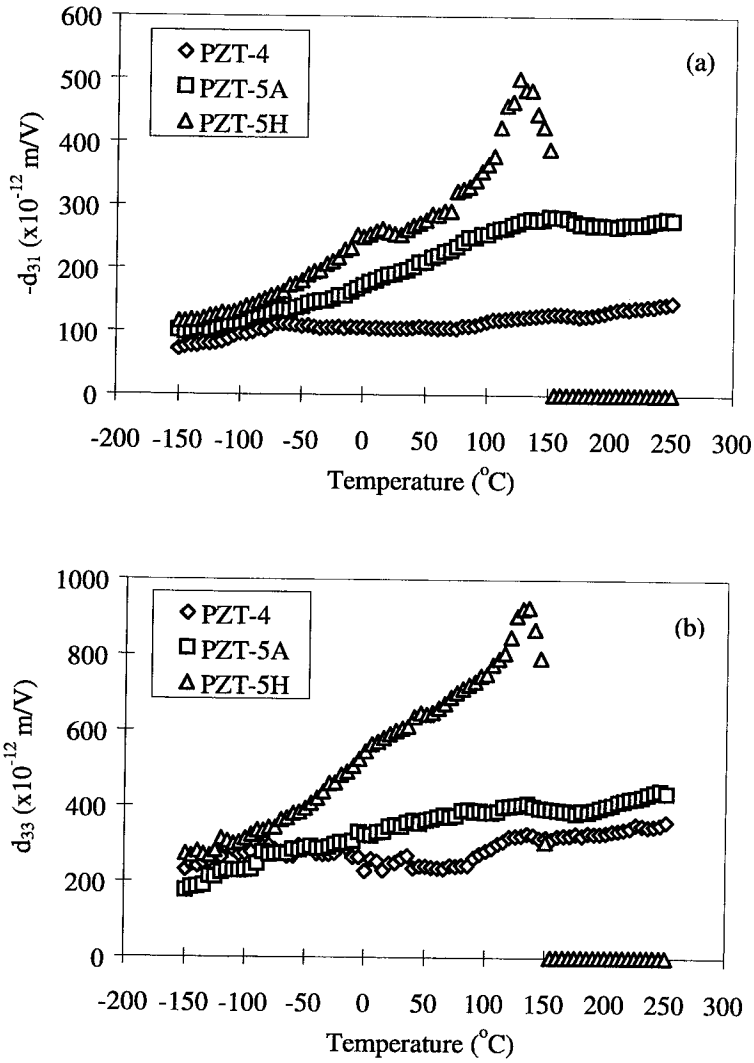

Figure 11. Typical (a) d_{31} and (b) d_{33} versus temperature behavior of PZT-4, PZT-5A, and PZT-5H ceramics.

Thermal Expansion

As shown in Figure 12, all of the piezoelectric specimens evaluated in this study showed some evidence of a phase transformation between 25 and 600°C. The PZT-4 specimen exhibited a change in the rate of expansion at approximately 310°C, whereas the PZT-5A and PZT-5H ceramics exhibited similar changes at 350 and 170°C respectively.

For the PZT-5H material, the temperature at which the rate of expansion changes correlates strongly with the T_c value of this composition. Although dielectric constant data was not obtained at temperatures greater than 250°C for the PZT-4 and PZT-5A ceramics, the thermal expansion data shown in Figure 12 provides a strong indication of the Curie points of these materials.

The PLZT-9/65/35 ceramics exhibited the largest thermal expansion of the materials tested. In this case, a change in the rate of thermal expansion was observed at approximately 275°C. This result suggests that a phase transformation other than the one indicated by the dielectric constant measurements takes place at this temperature.

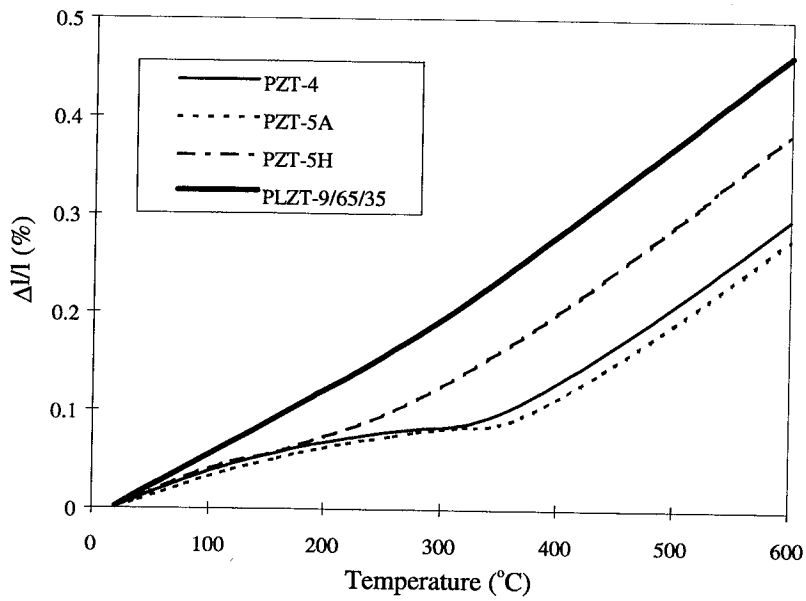

Figure 12. Relative change in length ($\Delta l/l_o$) versus temperature behavior of PZT-4, PZT-5A, PZT-5H, and PLZT-9/65/35 ceramics.

Mechanical Testing

Each test specimen fractured at a point between the inner two positions through which the mechanical load was applied. As shown in Table 3, the PZT-4 ceramics possessed the highest average MOR value, followed by the PZT-5A, PLZT-9/65/35, and PZT-5H compositions, respectively. All of the specimens tested in this work exhibited a MOR value that was within 10% of the average value for that composition.

Table 3. Modulus of Rupture (MOR) data for PZT-based ceramics.

Composition	Average MOR (MPa)
PZT-4	95.2
PZT-5A	81.8
PZT-5H	61.5
PLZT-9/65/35	69.3

Discussion

All of the materials evaluated in this investigation were found to possess properties that are suitable for use in aircraft and spacecraft systems. The selection of candidate materials for use in these systems is, however, strongly dependent upon the operational conditions under which the device will be employed. This is particularly important when selecting materials for low temperature (i.e., < -50°C) or high temperature (i.e., >150°C) applications.

Of the materials evaluated in this work, the PZT-5H ceramics were found to possess the highest $|d_{31}|$ and d_{33} coefficients at 25°C, followed by the PZT-5A and PZT-4 compositions, respectively. Although the PZT-5H ceramics exhibit the highest room temperature piezoelectric properties, this composition has a T_C value of 170°C which can be a limiting factor in applying this material in systems such as jet engines that could expose the actuator to temperatures above its Curie point.

Alternatively, both the PZT-4 and PZT-5A ceramics possess T_c values in excess of 300°C. The higher Curie temperatures of these materials make them more appropriate selections for higher-temperature applications. Although both of these compositions possess relatively high T_C values, the resistivity of PZT-4 decreases significantly above 120°C and it may, therefore, not be an attractive alternative for use above 100°C under high electric-field conditions. Near room temperature, however, PZT-4 has many useful characteristics, the most important of which is the retention of its polarization state over time when activated continuously using a large electric field [1].

The selection of actuator materials for low-temperature applications also requires careful consideration. In this work, the $|d_{31}|$ and d_{33} values of PZT-4 decreased less than 10% when cooled from room temperature to -150°C. Conversely, the d constants of both PZT-5A and PZT-5H decreased by approximately 50% when cooled over the same temperature interval. The relative stability of the properties of the PZT-4 ceramics between -150 and 25°C suggests that this material is a good candidate for some cryogenic applications. However, additional testing should be performed before this material is selected for use at temperatures below -150°C.

In addition to the temperature dependency of the piezoelectric properties, the dielectric constants of these materials must also be considered when evaluating candidate materials. In many aerospace systems, the power required to operate a device is a critical design issue. As shown below, the power consumed during the sinusoidal operation of a piezoelectric actuator is directly proportional to the capacitance of the device by the relation [25]:

$$P = \pi \cdot C \cdot f \cdot U^2 \tag{13}$$

where P is the power consumed (Watts), C is the capacitance of the actuator (Farads), f is the operational frequency (Hertz), and U is the peak-to-peak operational voltage ($V_{p\text{-}p}$). Thus, the selection of a material

with good piezoelectric properties must be weighed against the power consumed by the device to ensure that the power budget for the complete system is maintained.

The design of an optical positioning device for a space-based spectrometer system is a typical example of such a design trade-off. In a report by Wise et al. [26], the power consumed by similarly-sized PZT-5A and PZT-5H high-displacement RAINBOW actuator stacks was compared. In that study, PZT-5A stacks were found to meet the system's performance specifications while consuming 0.7 Watts of power whereas the PZT-5H stacks required 1.8 Watts of continuous power when operated at 1 Hz. As shown in Equation 13, the influence of the piezoelectric composition selected would become more pronounced if the actuator were required to operate at higher frequencies than those used in the system described in that study.

Over the course of this investigation, the properties of four PZT-based ceramics were evaluated between -150 to 250°C, and the temperature-dependent properties of these materials were related to existing aerospace applications of these materials. In addition to the four compositions evaluated herein, several other piezoelectric and electrostrictive compositions also exist which may possess properties that are more appropriate for a given set of design parameters. As such, the initial selection of candidate materials should not be limited only to those evaluated herein.

Conclusions

The dielectric, ferroelectric, and piezoelectric properties of three piezoelectric ceramics (PZT-4, PZT-5A, and PZT-5H) and one electrostrictive ceramic (PLZT-9/65/35) were measured over a temperature range of -150 to 250°C. Additionally, the thermal expansion characteristics of each composition were measured from 25 to 600°C, and the moduli of rupture were measured at 25°C. As the materials were heated above room temperature, PLZT-9/65/35 and PZT-5H were found to possess T_c values of 71 and 170°C, respectively. Neither the PZT-4 nor the PZT-5A ceramics exhibited a dielectric constant maxima below 250°C. Thermal expansion data indicate that these materials undergo phase transformations at 310 and 350°C, respectively.

All of the ceramic materials evaluated exhibited their maximum P_R values between 0 and 50°C. When cooled to -150°C, however, the polarization properties decreased to approximately 10% of the room temperature value for each composition. When heated above room temperature, the PLZT-9/65/35 and PZT-5H ceramics exhibited paraelectric P-E behaviors above their respective Curie points. The P-E behavior of the PZT-4 ceramics was influenced by the conductive nature of this composition above 120°C, whereas the PZT-5A ceramics exhibited square ferroelectric hysteresis loops, albeit with decreased E_c values, up to 250°C.

The PZT-5H ceramics exhibited the largest piezoelectric coefficients at room temperature, followed by the PZT-5A and PZT-4 compositions, respectively. When cooled to -150°C, the piezoelectric properties of the PZT-4 ceramics were found to remain relatively stable whereas the performance of the PZT-5A and PZT-5H materials decreased by approximately 50%. Conversely, when heated to 250°C, the PZT-5A ceramics possessed the largest piezoelectric properties. The PZT-4 specimens also exhibited strong piezoelectric resonances above room temperature. PZT-5H exhibited the largest piezoelectric properties up to its Curie point (170°C). Above this temperature, however, no resonances were observed, thus indicating that the specimens had been thermally de-poled.

All four of the materials evaluated in this study possess properties that are suitable for use in some

aerospace applications. These findings indicate, however, that careful consideration must be made in order to select optimum materials for a given set of operational conditions. This is particularly evident when choosing materials for either low-temperature (i.e., < -50°C) or high-temperature (i.e., >150°C) applications where the properties of the various materials deviate significantly from their room temperature behaviors.

References

1. B. Jaffe, W.R. Cook, and H. Jaffe, *Piezoelectric Ceramics*, New York: Academic Press, Inc., 1971.

2. G.H. Haertling, "Piezoelectric and Electrooptic Ceramics," pp. 139-225 in *Ceramic Materials for Electronics*, edited by R.C. Buchanan, New York: Marcel Dekker, Inc., 1986.

3. E.F. Crawley, "Intelligent Structures for Aerospace: A Technology Overview and Assessment," *AIAA Journal*, **32** [8] 1689-99, 1994.

4. S.S. Rao and M. Sunar, "Piezoelectricity and Its Use in Disturbance Sensing and Control of Flexible Structures: A Survey," *Applied Mechanics Reviews*, **47** [4] 113-123, 1994.

5. R.G. Loewy, "Recent Developments in Smart Structures with Aeronautical Applications," *Smart Materials and Structures*, **6** R11-R42, 1997.

6. R.E. Newnham and G.R. Ruschau, "Smart Electroceramics," *Journal of the American Ceramic Society*, **74** [3] 463-80, 1991.

7. K.B. Lazarus, E.F. Crawley, and J.D. Bohlmann, "Static Aeroelastic Control Using Strain Actuated Adaptive Structures," *Journal of Intelligent Material Systems and Structures*, **2** [3] 386-410, 1991.

8. D.L. Palumbo, S.L. Padula, K.H. Lyle, J.H. Cline and R.H. Cabell, "Performance of Optimized Actuator and Sensor Arrays in an Active Noise Control System," NASA TM 110281, 1996.

9. J. Heeg, "Analytical and Experimental Investigation of Flutter Suppression by Piezoelectric Actuation", NASA TP 3241, 1993.

10. R.W. Moses, "Vertical Tail Buffeting Alleviation Using Piezoelectric Actuators - Some Results of the Actively Controlled Response of Buffet-Affected Tails (ACROBAT) Program," NASA TM 110336, 1997.

11. P.P Friedman and T.A. Millott, "Vibration Reduction in Rotorcraft Using Active Control: A Comparison of Various Approaches," *Journal of Guidance, Control, and Dynamics*, **18** 664-73, 1994.

12. S.R. Hall and E.F. Prechtl, "Development of a Piezoelectric Servoflap for Helicopter Rotor Control," *Smart Materials and Structures*, **5** 26-34, 1996.

13. J. Shaw and N. Albion, "Active Control of the Helicopter Rotor for Vibration Reduction," *Journal of the American Helicopter Society*, **30** 3-20, 1981.

14. A.J. Butterfield and S.E. Woodard, "Measured Spacecraft Instrument and Structural Interactions," *Journal of Spacecraft and Rockets*, **33** [4] 556-62, 1996.

15. W.L. Grantham, "NASA Future Mission Needs and Benefits of Controls-Structures Interaction Technology," NASA TM 104034, 1991.

16. S. Zhou, C. Liang, and C.A. Rogers, "Dynamic Design and Stress Characteristics of Integrated Piezoelectric Patch Actuators," pp. 1360-74 in *Proceedings of the Second International Conference on Intelligent Materials (ICIM '94)*, edited by C.A. Rogers and G.G. Wallace, 1994.

17. S. Zhou, C. Liang, and C.A. Rogers, "Integration and Design of Piezoelectric Patch Actuators," *Journal of Intelligent Material Systems and Structures*, 6 [1] 125-33, 1995.

18. D. Shalev and J. Aboudi, "Coupled Micro to Macro Analysis of a Composite That Hosts Embedded Piezoelectric Actuators," *Journal of Intelligent Material Systems and Structures,* **7** [1] 15-25, 1996.

19. D.B. Koconis, L.P. Kollar, and G.S. Springer, "Shape Control of Composite Plates and Shells with Embedded Actuators, I. Voltages Specified," *Journal of Composite Materials*, **28** [5] 415-58, 1994.

20. D.B. Koconis, L.P. Kollar, and G.S. Springer, "Shape Control of Composite Plates and Shells with Embedded Actuators, II. Desired Shape Specified," *Journal of Composite Materials*, **28** [3] 262-85, 1994.

21. J.L Fanson, E.H. Anderson, and D. Rapp, "Active Structures for Use in Precision Control of Large Optical Systems," *Optical Engineering*, **29** [11] 1320-27, 1990.

22. "IRE Standards on Piezoelectric Crystals: Measurements of Piezoelectric Ceramics, 1961," *Proceedings of the IRE*, **49**, 1161-69, 1961.

23. "IEEE Standard on Piezoelectricity," ANSI/IEEE Standard 176-1987, 1987.

24. J.T. Jones and M.F. Berard, *Ceramics: Industrial Processing and Testing*, Ames, Iowa: Iowa State University Press, 1972.

25. Anon., "Piezo Guide: Piezo Positioning Technology Part 1," Catalogue PZ 36E. *Products for Micropositioning*, Physik Instrumente Catalogue 108-12/90.14.

26. S.A. Wise, R.C. Hardy, and D.E. Dausch, "Design and Development of an Optical Path Difference Scan Mechanism for Fourier Transform Spectrometers Using High-Displacement RAINBOW Actuators," in Industrial and Commercial Applications of Smart Structures Technologies, edited by J.M. Sater, *Proceedings of SPIE*, **3044** 342-349, 1997.

REPORT DOCUMENTATION PAGE

Form Approved
OMB No. 0704-0188

1. AGENCY USE ONLY (*Leave blank*)

2. REPORT DATE
September 1998

3. REPORT TYPE AND DATES COVERED
Contractor Report

4. TITLE AND SUBTITLE
Properties of PZT-Based Piezoelectric Ceramics Between -150 and 250C

5. FUNDING NUMBERS
C NAS1-96014
WU 522-32-11-02

6. AUTHOR(S)
Matthew W. Hooker

7. PERFORMING ORGANIZATION NAME(S) AND ADDRESS(ES)
Lockheed-Martin Engineering & Sciences Co.
Mail Stop 371
NASA-Langley Research Center
Hampton, VA 23681

8. PERFORMING ORGANIZATION REPORT NUMBER

9. SPONSORING/MONITORING AGENCY NAME(S) AND ADDRESS(ES)
National Aeronautics and Space Administration
Langley Research Center
Hampton, VA 23681-2199

10. SPONSORING/MONITORING AGENCY REPORT NUMBER
NASA/CR-1998-208708

11. SUPPLEMENTARY NOTES
Langley Technical Monitor: Stephanie A. Wise
Final Report

12a. DISTRIBUTION/AVAILABILITY STATEMENT
Unclassified-Unlimited
Subject Category 76 Distribution: Standard
Availability: NASA CASI (301) 621-0390

12b. DISTRIBUTION CODE

13. ABSTRACT (*Maximum 200 words*)

The properties of three PZT-based piezoelectric ceramics and one PLZT electrostrictive ceramic were measured as a function of temperature. In this work, the dielectric, ferroelectric polarization versus electric field, and piezoelectric properties of PZT-4, PZT-5A, PZT-5H, and PLZT-9/65/35 were measured over a temperature range of -150 to 250C. In addition to these measurements, the relative thermal expansion of each composition was measured from 25 to 600C and the modulus of rupture of each material was measured at room temperature. This report describes the experimental results and compares and contrasts the properties of these materials with respect to their applicability to intelligent aerospace systems.

14. SUBJECT TERMS
piezoelectric, PZT, PLZT, temperature

15. NUMBER OF PAGES
30

16. PRICE CODE
AO3

17. SECURITY CLASSIFICATION OF REPORT	18. SECURITY CLASSIFICATION OF THIS PAGE	19. SECURITY CLASSIFICATION OF ABSTRACT	20. LIMITATION OF ABSTRACT
Unclassified	Unclassified	Unclassified	